Supporting Information

Kinetics of equilibrium passive sampling of organic chemicals with polymers in diverse mammalian tissues

Andreas Baumer, Sandra Jäsch, Nadin Ulrich, Ingo Bechmann, Julia Landmann, Beate I. Escher*

Andreas Baumer – *Department Cell Toxicology, Helmholtz Centre for Environmental Research– UFZ, 04318 Leipzig, Germany*

Nadin Ulrich – *Department Analytical Environmental Chemistry, Helmholtz Centre for Environmental Research– UFZ, 04318 Leipzig, Germany*

Sandra Jäsch – *Department Analytical Environmental Chemistry, Helmholtz Centre for Environmental Research– UFZ, 04318 Leipzig, Germany*

Ingo Bechmann – *Institute of Anatomy, University of Leipzig, 04103 Leipzig, Germany*

Julia Landmann – *Institute of Anatomy, University of Leipzig, 04103 Leipzig, Germany*

Beate I. Escher – *Department Cell Toxicology, Helmholtz Centre for Environmental Research– UFZ, 04318 Leipzig, Germany and Environmental Toxicology, Centre for Applied Geosciences, Eberhard Karls University Tübingen, 72076 Tübingen, Germany*

*Corresponding Author**:** Beate I. Escher. Tel. +49 341 235 1244. Email: beate.escher@ufz.de.

Table of Contents

Table S1. Chemicals used in this study and their identifiers and basic physicochemical properties – see separate excel file.

Chemical identifiers include the CAS and DTXSID numbers. Chemicals were classified in chemical classes (pesticides, OCP = organochlorine pesticides, OP = organophosphate insecticides, PAH = polycyclic aromatic hydrocarbons, PBDE = polybrominated diphenylethers (brominated flame retardants), OFR = organophosphorus flame retardants). Listed are octanol-water partition constants logK_{ow}, PDMS-water partition constants log$K_{PDMS/water}$, liposome-water partition constant log$K_{liposome/water}$, storage lipid-water partition constant log$K_{storage\ lipid/water}$, bovine serum albumin-water partition constants (BSA) log$K_{BSA/water}$, chicken muscle protein-water partition constants log$K_{muscle\ protein/water}$. Experimental values were given preferences and missing values were filled by Linear Solvation Energy Relationship (LSER)[1] or, if no descriptors for LSER were available, by Quantitative Structure Activity relationships (QSAR) using the logK_{ow} as descriptor.[2-4] In addition the $K_{lipid/water}$ (adipose tissue) are listed which were calculated from $K_{lipid/PDMS}$ (adipose tissue) (Table 1) and $K_{PDMS/water}$ with eq. 11.

Table S2. Internal standards for quantification used in this study.

Internal standard (ISTD)	Abbreviation	Supplier
Tris-(2-chloroethyl phosphate)-d_{12}	TCEP-d_{12}	Sigma-Aldrich
$^{13}C_3$-Atrazine	$^{13}C_3$-Atrazine	Cambridge Isotope Laboratories
Diazinon-d_{10}	Diazinon-d_{10}	Campro Scientific
$^{13}C_{12}$-2,4,4'-Trichlorobiphenyl	$^{13}C_{12}$-PCB28	Cambridge Isotope Laboratories
Chlorpyrifos-methyl-d_6	Chlorpyrifos-M-d_6	Dr. Ehrenstorfer
Metolachlor-d_6	Metolachlor-d_6	Campro Scientific
p,p'-Dichlorodiphenyltrichloroethane-d_8	*p,p'*-DDT-d_8	Sigma-Aldrich
$^{13}C_{12}$-2,2',3,4,4',5'-Hexachlorobiphenyl	$^{13}C_{12}$-PCB138	Cambridge Isotope Laboratories
Triphenyl phosphate-d_{15}	TPP-d_{15}	Sigma-Aldrich
Etofenprox-d_5	Etofenprox-d_5	Dr. Ehrenstorfer
Benzo[*a*]pyrene-d_{12}	B[*a*]P-d_{12}	Dr. Ehrenstorfer
Chrysene-d_{12}	Chrysene-d_{12}	Dr. Ehrenstorfer
$^{13}C_{12}$-2,2',4,4'-Tetrabromodiphenyl ether	$^{13}C_{12}$-BDE47	Cambridge Isotope Laboratories
$^{13}C_{12}$-2,2',4,4',5,5'-Hexabromodiphenyl ether	$^{13}C_{12}$-BDE153	Cambridge Isotope Laboratories

Table S3. Chemicals and solvents used in this study.

Chemical	Abbreviation	Supplier
Bovine serum albumin	BSA	Sigma-Aldrich
1-Palmitoyl-2-oleoyl-sn-glycero-3-phosphocholine	POPC	Avanti Polar Lipids
Triolein	TR	Sigma-Aldrich
Sodium dodecyl sulphate	SDS	Sigma-Aldrich
Cyclohexane	CH	Merck (GC grade)
2-Propanol	IPA	Merck (GC grade)
Ethyl acetate	EA	Honeywell (LC grade)
Ultrapure water	H_2O	Milli-Q Water Purification System Merck-Millipore (Darmstadt, Germany)

Text S1. Determination of total lipid content.

Total lipid content was gravimetrically determined by employing a modified solvent extraction method with cyclohexane (CH), 2-propanol (IPA) and water after Smedes[5] and was previously described by Baumer et al.[6] Briefly, 50 to 500 mg of tissue or blood were extracted in triplicates employing a mixture of water, CH and IPA (1.47 mL water, 1.3 mL of CH and 1 mL of IPA) in glass extraction vials and vortexed for 30 s. After centrifugation at 4000 rpm for 5 min, the upper CH phase was pipetted using a glass Pasteur pipette (Brand, Wertheim, Germany) in a pre-weighted collection vial. Extraction was repeated three times by adding 1.13 mL of CH and 0.175 mL of IPA after each cycle. The combined solvent extracts were blown down under a gentle stream of nitrogen and further dried in a desiccator over silica gel overnight. The collection vials with the dry lipid residue were weighted on microbalance (METTLER TOLEDO, Gießen, Germany). Total lipid content was then determined gravimetrically and was corrected to negative and positive controls. Besides the negative (BSA) and positive (TR and POPC) controls, methods blanks (water instead of sample matrix) and solvent blanks (CH and IPA) were included in each extraction batch to check for contamination of the used glass ware and solvents.

Text S2. Determination of total protein content.

Total protein content was determined colorimetrically using Thermo Scientific™ Pierce™ BCA Protein Assay Kit (Thermo Scientific, USA) on 96 well-microplates. The test was carried out according to the test protocol provided by Thermo Scientific. The addition of sodium dodecyl phosphate (SDS) to T-PER reagent was necessary due to the elimination of matrix effects because of interfering lipids. 0.5 to 1 g tissue was mixed with 5 to 10 mL of a detergent containing protein extraction reagent (T-PER, Thermo Scientific, USA) with 2% sodium dodecyl sulphate (SDS). After centrifugation at 4000 rpm for 5 min, the supernatant was used for the determination of total protein content. Blood samples were diluted with the T-PER reagent and the resulting solution was used for quantitation of total proteins. 200 µL working reagent (consisting of BCA Reagent A and BCA Reagent B in a ratio of 50:1 (V/V)) were pipetted onto 10 to 25 µL unknown sample or calibration standard (four replicates each), which were obtained from the T-PER extraction step or by preparation of the calibration standard, respectively. The solution was mixed vigorously on a microplate vortexer (VXR basic, IKA, Staufen, Germany) with 800 rpm for 30 s. Air bubbles which may have formed during the shaking process caused by the detergent were eliminated using a blow-dryer. After two hours of incubation in the dark at room temperature, absorbance was measured at 562 nm with a micro-plate

reader TECAN Infinite M1000 Pro (TECAN, Männedorf, Switzerland). Multiple measurements at different positions in each well were conducted excluding possible precipitations by present matrix components. Quantitation of total protein content was carried out using the linear regression equation of the calibration curve with BSA as standard (range 20 – 2000 µg mL^{-1}) and T-PER as blank.

Text S3. Spiking of tissue with a defined mixture of 40 chemicals.

The required amount of tissue [g] for the kinetic experiments was weighed in a beaker or blood [mL] was directly filled in the 4 mL experiment vials. The calculated volume of the spiking solution was carefully pipetted onto the tissue or blood. After the ethyl acetate was evaporated under the fume hood, the tissue was mixed with a spatula and the beaker was sealed with aluminium foil and parafilm and vials with spiked blood were closed with a PTFE containing lid and gently mixed. The spiked tissues and blood were stored overnight in a fridge at 4 °C in the dark to ensure equal distribution of the chemicals before the start of the kinetic experiments.

For the tissues, a spike solution containing all compounds with a concentration of 40 ng μL^{-1} in ethyl acetate was prepared from the 1 mg mL^{-1} stock solutions. For blood, a spike solution with a concentration of 4 ng μL^{-1} in ethyl acetate was prepared. In the first experiments, the same concentrations were spiked for each chemical, in the repeat experiments, there were individual spikes for each chemical due to differences in depletion of the tissue by the PDMS extraction. The molar amount spiked per chemicals is detailed in Tables S6, S7, S9 and S11.

Adipose tissue: Exp.1: 4000 ng g^{-1} adipose tissue (all chemicals)

Exp.2: Hydrophilic chemicals: 300 – 1000 ng $g_{adipose\ tissue}^{-1}$ (individual spike for each chemical)

Exp.2: Hydrophobic chemicals: 2000 – 8000 ng $g_{adipose\ tissue}^{-1}$ (individual spike for each chemical)

Liver: Exp. 1: 292 ng $g_{liver\ tissue}^{-1}$ (all chemicals)

Exp. 2: 200 ng $g_{liver\ tissue}^{-1}$ (all chemicals)

Exp. 3: 267 ng $g_{liver\ tissue}^{-1}$ (all chemicals)

Exp. 4: Range: 100 – 500 ng $g_{liver\ tissue}^{-1}$ (individual spike for each chemical)

Brain: Exp. 1: 200 ng $g_{brain\ tissue}^{-1}$ (all chemicals)

Exp. 2: 160 ng $g_{brain\ tissue}^{-1}$ (all chemicals)

Exp. 3: Range: 20 – 600 ng $g_{brain\ tissue}^{-1}$ (individual spike for each chemical)

Blood: Exp. 1: 18 ng mL^{-1} blood (all chemicals)

Exp. 2: 15 ng mL^{-1} blood (all chemicals)

Exp. 3: 27 ng mL^{-1} blood and 36 ng mL^{-1} blood (all chemicals)

Text S4: PDMS-to-tissue ratios.

PDMS-to-tissue ratios used in the passive sampling experiment were calculated based on the negligible depletion criterion that less than 5% of the total molar amount of chemical is extracted by PDMS ($n_{PDMS}/n_{tot} < 0.05$).[7] For this estimation, we assumed that all chemicals are associated to lipids, i.e., $n_{tot} = n_{lipid}$, which is not correct for lean tissue but serves as an approximation. The ratio of the mass of PDMS (m_{PDMS}) and the partition constants $K_{lipid/PDMS}$ multiplied by the mass of the lipid present in the tissue (m_{lipid}) should not exceed 5% (equation S1).

$$\frac{n_{PDMS}[mol]}{n_{lipid}[mol]} = \frac{m_{PDMS}[kg_{PDMS}]}{K_{lipid/PDMS}\,[kg_{PDMS}\ kg_{lipid}^{-1}] \times m_{lipid}\,[kg_{lipid}]} \leq 0.05 \qquad \text{(S1)}$$

The final PDMS-to-tissue ratios used in this study are described in the section "Passive sampling of tissues and blood" of the main text.

Blood was exhaustively extracted and therefore the ratio of PDMS to blood was increased as described by Jin and co-workers[8] for blood from marine turtles. The authors used approx. 1 g PDMS for the extraction of hydrophobic organic contaminants (HOCs) from 5 mL blood. We used the same ratio, but downscaled the volumes of both blood and PDMS. The final experiment consisted of approximately 400 mg PDMS and 2.2 mL blood.

Text S5: Preparation of PDMS.

To ensure that no residuals of impurities or monomers were left in the PDMS, the sheets were cleaned with Soxhlet extraction with ethyl acetate for 24 h. The purified PDMS sheets were stored at room temperature in brown DURAN® bottles covered with fresh ethyl acetate. Before the start of the passive sampling experiments, the PDMS was air dried for at least 2 h. During this time, the entire ethyl acetate evaporated and the initial mass of the PDMS before the start of the passive sampling experiments could be determined using a microbalance (METTLER-TOLEDO, Gießen, Germany).

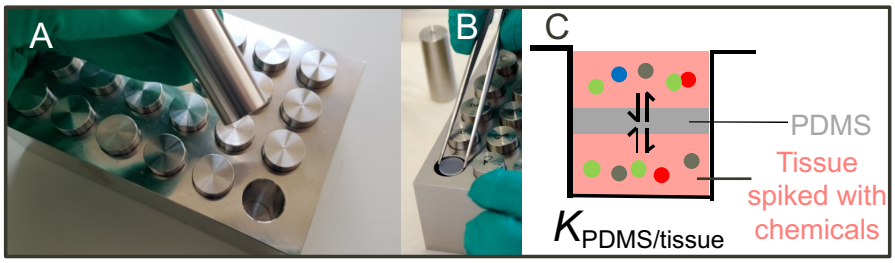

Figure S1. Static passive sampling experiments.

(A) Experimental set-up for static passive sampling experiments with adipose tissue using metal blocks. (B) Insertion of PDMS disk. (C) Illustration of the sandwiched PDMS disk between adipose tissue layers inside the cavities.

Figure S2. Dynamic sampling method for blood.

PDMS forming wings inside 4 mL vials placed on a roller mixer for exposure experiments with blood.

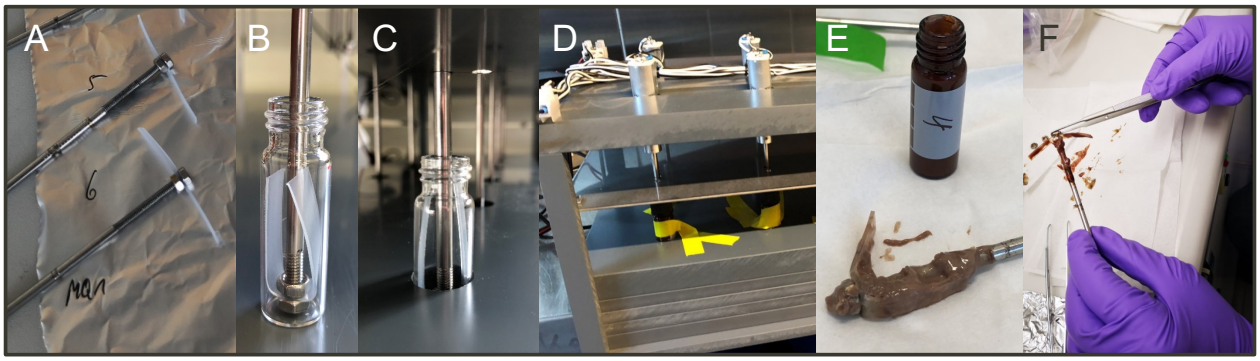

Figure S3. Dynamic sampling method for liver and brain.

(A) PDMS strips mounted and fixed on metal rods with screwing nuts before extraction. (B) and (C) PDMS strip serves as stirrer and sampler simultaneously. Note that experiments were carried it out brown glass vials, transparent glass was only used for the photos. (D) Vials filled with tissue and mounted PDMS on rods clamped in the mixing machine. Additional fixation using adhesive tapes of the vials avoided spinning of the vials. (E) PDMS strip retrieved from vial after experiment. (F) Dismounting PDMS strips from metal using tweezers followed by cleaning of the sampler and extraction.

Text S6. Additional information on the instrumental analysis.

A GC-MS/MS method with direct sample introduction (DSI) developed by Baumer et al.[6] was employed with minor modifications. Helium (6.0 purity) was used as carrier gas in constant flow mode at a flow rate 1.3 mL min^{-1} and the solvent delay was set at 7.5 min. The MS transfer line was kept at 250 °C, the ion source at 230 °C and both quadrupoles were operated at 150 °C. Nitrogen was used as collision gas at a flow of 1.5 mL min^{-1}. Helium was used as quench gas at 2.25 mL min^{-1}. Two mass transitions under specific collision energies (CEs) for quantification and qualification were determined for each analyte (Table S4). A volume of 1 µL sample extract was injected into the thermodesorption unit (TDU) tubes with frit. During injection, the initial temperature of the TDU program was set to 30 °C. The helium flow was kept at 50 mL min^{-1} until the thermodesorption cycle was completed and the temperature of the TDU was raised to 300 °C at 720 °C min^{-1} (hold for 3 min). The transfer line of the TDU was set to 300 °C. The cold injection system (CIS) was operated in solvent vent mode with an empty baffled liner. During thermal desorption, the CIS temperature was set to -30 °C for cryofocussing. After finishing the thermal desorption cycle, the temperature of the injector was raised to 300 °C at 12 °C s^{-1} (3 min) ensuring a complete transfer of the analytes to the analytical column. Analytes were separated on a HP5-MS UI® capillary column (30 m length,

0.25 µm i.d., 0.25 µm film thickness, J&W Scientific, USA). The oven was programmed as follows: 60 °C (hold for 3 min) to 210 °C at 30 °C min^{-1} (hold for 5 min), to 240 °C at 3 °C min^{-1} and finally to 300 °C at 40 °C min^{-1} (hold for 5 min). Matrix extracts after PDMS sampling spiked with only isotopically labelled internal standard solution were used as blanks and showed no contamination. Matrix matched calibration mixtures of all analytes were prepared in concentrations of 20, 30, 50, 75, 150, 400, 1200 pg μL^{-1} in ethyl acetate. Data acquisition and instrument control was conducted with MassHunter– Data Acquisition (Agilent Technologies, USA) with an integrated Maestro (GERSTEL GmbH, Mülheim a. d. Ruhr, Germany). For data analysis MassHunter QQQ Quantitative Analysis (Version B.07.01 SP1, Agilent Technologies, USA) was used.

For the experiments with the bioassays, where only PCB126 was spiked to tissue, a GC-MSD method was applied on an Agilent 6890 GC with a 5973 Single Quadrupole MS (Agilent Technologies, USA). The MSD was operated in EI mode at 70 eV. Measurements were carried out using selected ion monitoring (SIM) with ions (*m/z*) 326.0 as quantifier and 254.0 as qualifier, respectively. 1 µL sample extract in ethyl acetate was injected in splitless mode into the Split/Splitless inlet at 250 °C. Chromatographic separation was performed on a DB 5-MS UI® capillary column (30 m length, 0.25 µm i.d., 0.25 µm film thickness, J&W Scientific, USA). The oven was programmed as follows: 60 °C (held for 1 min) to 210 °C at 30 °C min^{-1} (held for 1 min), to 260 °C at 10 °C min^{-1} (held for 3 min) and finally to 300 °C at 40 °C min^{-1} (held for 3 min) which resulted in a total run time of 19 min. The retention time (t_R) of PCB126 was 12.64 min. Helium (6.0 purity) was used as carrier gas in constant flow mode at 1.2 mL min^{-1} and the solvent delay was set to 6.0 min. The MS transfer line was kept at 250 °C, the ion source at 230 °C and the quadrupole at 150 °C. To circumvent matrix effects caused by the low amount of co-extracted matrix components, quantification was carried out with a matrix matched calibration in the range of 2.5 pg μL^{-1} to 500 pg μL^{-1}. The concentration present in the extract, equal to the concentration measured in the PDMS (C_{PDMS} [mol g_{PDMS}^{-1}]) was derived by the calculated mass of PCB126 from the linear regression divided by the mass of the used PDMS. MS ChemStation software (Agilent Technologies, USA) was used both for instrument control (Data Acquisition Software) and data evaluation (Data Analysis Software) for the GC-MSD.

147 **Table S4. Retention times (t_R), MRM transitions of quantifier and qualifier ions, and their collision**
148 **energies (CE) for each analyte.**

Analyte	Retention time t_R [min]	Quantifier ion (*m/z*)	CE (eV)	Qualifier ion (*m/z*)	CE (eV)	ISTD for quantitation
Atrazine	8.30	214.8 → 58.0	15	214.9 → 200.1	5	$^{13}C_3$-Atrazine
TCEP	8.31	248.8 → 62.9	40	248.9 → 125.0	15	TCEP-d_{12}
Lindane	8.46	180.8 → 144.9	15	218.8 → 182.9	5	$^{13}C_{12}$-PCB28
Diazinon	8.55	303.8 → 179.1	20	198.7 → 93.0	20	Diazinon-d_{10}
PCB28	9.25	255.7 → 186.0	30	255.7 → 221.0	15	$^{13}C_{12}$-PCB28
Chlorpyrifos-M	9.35	285.6 → 93.0	20	124.9 → 78.9	5	Chlorpyrifos-M-d_6
Heptachlor	9.56	271.7 → 236.9	15	236.7 → 118.8	40	$^{13}C_{12}$-PCB28
PCB52	9.87	219.9 → 185.0	20	291.6 → 257.0	10	$^{13}C_{12}$-PCB28
Metolachlor	10.24	237.8 → 162.1	20	161.8 → 133.1	20	Metolachlor-d_6
Aldrin	10.27	262.8 → 227.9	20	292.7 → 222.0	30	$^{13}C_{12}$-PCB28
Chlorpyrifos-E	10.31	196.8 → 168.9	15	313.7 → 257.9	15	Chlorpyrifos-M-d_6
Bromophos-M	10.76	330.7 → 315.9	20	330.7 → 93.0	40	Chlorpyrifos-M-d_6
Cybutryne	11.43	181.9 → 109.1	20	252.7 → 182.0	20	$^{13}C_3$-Atrazine
Fipronil	11.44	366.7 → 213.1	40	366.8 → 255.0	40	Metolachlor-d_6
Bromophos-E	12.01	358.7 → 302.9	15	330.7 → 302.9	5	Chlorpyrifos-M-d_6
PCB101	12.16	325.6 → 256.0	30	325.6 → 291.0	15	$^{13}C_{12}$-PCB28
p,p'-DDE	13.15	245.7 → 176.0	30	317.6 → 248.0	20	*p,p'*-DDT-d_8
Chlorfenapyr	14.10	327.8 → 247.1	20	246.8 → 75.0	40	Metolachlor-d_6
PCB118	14.33	325.6 → 256.0	30	253.7 → 184.0	40	$^{13}C_{12}$-PCB138
BDE28	14.39	245.8 → 139.0	30	405.8 → 246.0	15	$^{13}C_{12}$-BDE47

149

150

Table S4. Continued.

Analyte	Retention time t_R [min]	Quantifier ion (*m/z*)	CE (eV)	Qualifier ion (*m/z*)	CE (eV)	ISTD for quantitation
p,p'-DDD	14.63	234.7 → 165.1	40	234.7 → 199.0	20	*p,p'*-DDT-d_8
PCB114	14.72	325.6 → 256.0	30	253.7 → 184.0	40	$^{13}C_{12}$-PCB138
PCB153	15.10	359.6 → 290.0	40	359.6 → 324.9	15	$^{13}C_{12}$-PCB138
p,p'-DDT	15.98	234.7 → 165.0	30	234.7 → 199.0	20	*p,p'*-DDT-d_8
PCB138	16.10	359.7 → 289.9	30	359.7 → 324.9	15	$^{13}C_{12}$-PCB138
PCB126	16.44	325.6 → 256.0	30	253.7 → 184.0	40	$^{13}C_{12}$-PCB138
TPP	16.76	325.6 → 169.0	40	214.8 → 168.0	15	TPP-d_{15}
Chrysene	17.75	114.0 → 101.0	10	227.8 → 202.1	30	Chrysene-d_{12}
PCB156	17.95	359.6 → 289.9	30	289.7 → 255.0	30	$^{13}C_{12}$-PCB138
Methoxychlor	18.14	226.7 → 169.1	30	226.8 → 184.1	20	*p,p'*-DDT-d_8
PCB180	18.46	393.6 → 323.9	40	393.6 → 358.9	15	$^{13}C_{12}$-PCB138
BDE47	18.52	485.8 → 325.9	20	325.8 → 219.0	30	$^{13}C_{12}$-BDE47
TMPP	19.13	276.8 → 179.1	15	368.0 → 277.1	5	TPP-d_{15}
BDE100	19.89	563.8 → 403.8	40	405.8 → 296.9	40	$^{13}C_{12}$-BDE153
PCB194	19.90	429.6 → 359.8	40	429.6 → 394.8	15	$^{13}C_{12}$-PCB138
BDE99	20.22	563.8 → 403.8	20	405.8 → 296.9	40	$^{13}C_{12}$-BDE153
Etofenprox	20.64	162.9 → 107.1	20	162.9 → 135.1	15	Etofenprox-d_5
B[*a*]P	20.69	126.1 → 113.1	5	251.8 → 226.1	30	B[*a*]P-d_{12}
PCB209	20.83	497.6 → 427.8	40	497.6 → 462.8	15	$^{13}C_{12}$-PCB138
BDE153	21.83	643.7 → 483.8	20	483.7 → 404.8	20	$^{13}C_{12}$-BDE153

153 **Table S5. Retention times (t_R), MRM transitions of quantifier and qualifier ions, and their collision**
154 **energies (CE) for each internal standard.**

ISTD	Retention time t_R [min]	Quantifier ion (*m/z*)	CE (eV)	Qualifier ion (*m/z*)	CE (eV)
TCEP-d_{12}	8.22	261.0 → 66.9	25	261.0 → 131.0	10
$^{13}C_3$-Atrazine	8.28	217.9 → 203.1	5	217.9 → 176.1	5
Diazinon-d_{10}	8.49	314.0 → 183.1	15	314.0 → 199.1	5
$^{13}C_{12}$-PCB28	9.23	267.8 → 198.1	35	197.9 → 163.1	25
Chlorpyrifos-M-d_6	9.29	291.8 → 99.1	35	291.8 → 273.9	20
Metolachlor-d_6	10.18	241.9 → 166.1	15	165.1 → 134.1	15
p,p'-DDT-d_8	15.86	242.8 → 173.1	35	242.8 → 208.1	15
$^{13}C_{12}$-PCB 138	16.08	371.8 → 301.9	35	371.8 → 337.0	15
TPP-d_{15}	16.60	222.9 → 176.0	25	340.8 → 243.2	15
Etofenprox-d_5	20.61	167.9 → 108.1	20	167.9 → 136.1	15
B[*a*]P-d_{12}	20.65	132.1 → 118.1	15	263.2 → 236.2	40
Chrysene-d_{12}	17.65	120.1 → 106.1	15	239.9 → 212.2	40
$^{13}C_{12}$-BDE47	18.50	497.8 → 337.9	20	337.8 → 230.0	30
$^{13}C_{12}$-BDE153	21.82	655.9 → 495.9	20	494.8 → 415.5	20

155

156

Text S7. Additional information on bioassay experiments after static and dynamic equilibrium passive sampling with liver tissue.

AhR CALUX cells were obtained by courtesy of Michael Denison, UC Davis, USA. The procedure of culturing the cells and the AhR CALUX assay was published previously.[9-11] Thirty µL of cell suspension (containing 3250 cells) were plated in each well of a 384-well microtiter plate (black with clear bottom, polystyrene, BioCoat, #356663, Corning, Maine, USA). For this purpose, a Multiflow Dispenser (Biotek, Vermont, USA) was used. The cells were incubated at 37 °C and 5% CO_2 for 24 h. Assay medium (Thermo Fisher Scientific, USA) consisted of 90% Dulbecco´s modified Eagle´s medium with Glutamax and 10% fetal bovine serum (FBS) supplemented with penicillin (100 U mL^{-1}) and streptomycin (100 µg mL^{-1}).[10, 11]

Sample extracts in ethyl acetate gained from passive sampling experiments (details on passive sampling experiments see main text) were split equally into two vials (one vial for GC-MS analysis and one vial for bioassay). For the AhR CALUX, the ethyl acetate was exchanged to DMSO. This step was necessary, because the dosing was realized using a Tecan D300e Digital Dispenser (Tecan, Crailsheim, Germany) with DMSO as a compatible solvent. For the preparation of the 96-well dilution plates (clear, Corning, Maine, USA), 30 pL to 10 µL of the sample extracts dissolved in DMSO were pipetted into the preloaded medium achieving serial dilution of the desired concentration range.[10] Before dosing, the dilution plates were shaken on a plate mixer (IKA, Staufen, Germany) for 30 s at 800 rpm. Ten µL per well in 96 well dilution plates were transferred into 30 µL per well in the 384-well plate using a pipetting robot (Hamilton Microlab Star, Bonaduz, Schwitzerland).[10]

The cell confluency was measured both before and after dosing of 24 h incubation time (37°C and 5% CO_2) with an IncuCyte S3 live cell imaging system (Essen BioScience, Ann Arbor, Michigan, USA). The cyctotoxicity was evaluated from the measured cell confluency as described by Escher et al. (2019).[10]

The inhibitory concentration for 10% reduction of cell viability (IC_{10}) was derived from the slope of the linear concentration-response curve (linearity below 30% inhibition).[11, 12]

The concentration causing 10% effect (EC_{10}) relative to the maximum effect caused by the positive control from the linear portion of the concentration-response curve below 30% and below the IC_{10} was calculated using equation S2 and equation S3 was used for calculating the standard error (se) of the EC_{10}.[11, 12]

$$EC_{10} = \frac{10}{\text{slope}} \quad \text{(S2)}$$

$$se(EC_{10}) = \frac{10}{slope^2} \times se(slope) \quad \text{(S3)}$$

To compare the bioassays results with the measured concentration in the PDMS (C_{PDMS} [mol g_{PDMS}^{-1}]) from GC analysis, the bioanalytical equivalent concentration (BEQ) of PCB126 in PDMS (PCB126-EQ) [mol g_{PDMS}^{-1}] was derived by dividing the EC_{10} of the reference compound by the EC_{10} of the individual sample (equation S4).

$$\text{PCB126-EQ} = \frac{EC_{10}\ (\text{reference})}{EC_{10}(\text{sample})} \quad \text{(S4)}$$

The standard error (se) of the PCB126-EQ was calculated with equation S5.

$$se(\text{PCB126-EQ}) = \sqrt{\frac{1}{EC_{10}(\text{sample})^2} \cdot \times\ se(EC_{10}\ (\text{reference}))^2 + \frac{EC_{10}\ (\text{reference})^2}{EC_{10}(\text{sample})^4} \times se(EC_{10}\ (\text{sample}))^2} \quad \text{(S5)}$$

GraphPad Prism (Version 8.4, San Diego, CA, USA) was used for regression analysis and for graphing of the concentration-response curve.

Text S8. Equilibrium in adipose tissue.

Confirmation that equilibrium had been attained in adipose tissue was achieved by plotting the sum of the mass of each compound class [ng] against the mass of PDMS [mg] for four different thicknesses of PDMS polymer (0.25 mm (29 mg), 0.33 mm (52 mg), 0.63 mm (83 mg), and 1 mm (124 mg)).[7, 13] The group of polychlorinated biphenyls (PCB) included the following congeners: PCB28, PCB52, PCB101, PCB118, PCB138, PCB153, PCB180 and PCB194 (Figure S5A). diazinon, chlorpyrifos-E, chlorpyrifos-M, bromophos-E and bromophos-M were assigned to organophosphates (Figure S5B). Figure S5C shows organochlorine pesticides (DDD, DDE, DDT and methoxychlor, Figure 5C). Organophosphorus flame retardants (Figure S5D) consisted of TCEP, TPP and TMPP. Finally, the group of pesticides (Figure S5E) contained atrazine, metolachlor, fipronil, and chlorfenapyr. The linear regression in Figure S5 confirmed that equilibrium was reached after 96 h of sampling time for each compound class.

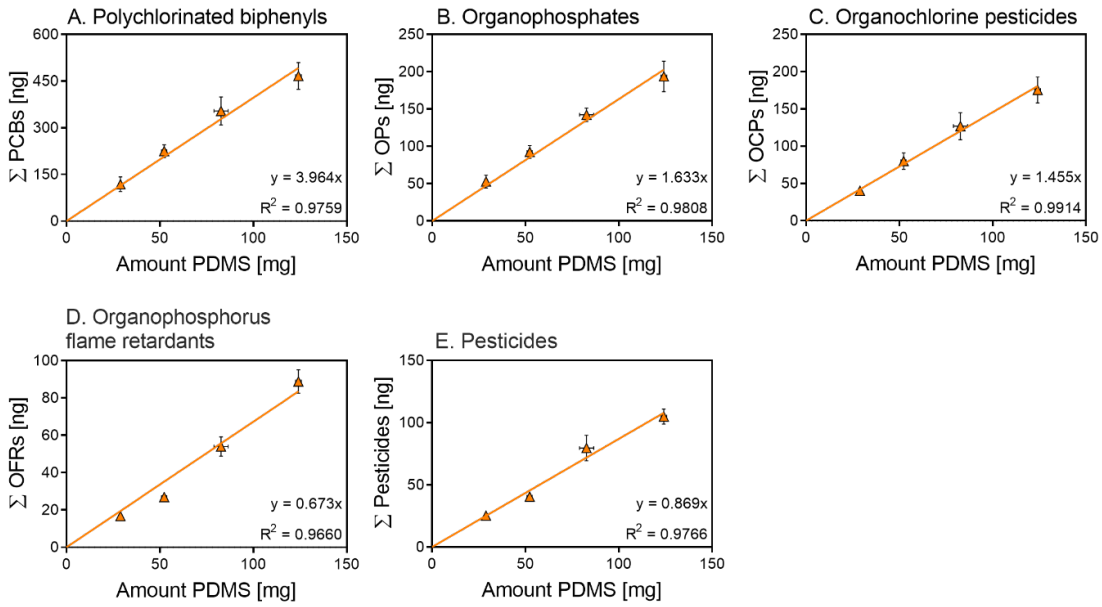

Figure S5. Sum of concentrations of the different chemical groups in PDMS of varying thickness.

Confirmation that equilibrium had been attained in adipose tissue was achieved by plotting the sum of the mass of each compound class [ng] against the mass of PDMS [mg] for four different thicknesses of PDMS polymer (0.25 mm (29 mg), 0.33 mm (52 mg), 0.63 mm (83 mg), and 1 mm (124 mg) expressed as weight equilibrium reached between adipose tissue and PDMS after 96 h sampling.

(A) Polychlorinated biphenyls, (B) organophosphates, (C) organochlorine pesticides, (D) organophosphorus flame retardants, (E) pesticides. In the diagrams, the means of triplicate samples with standard deviations and the linear regression through zero are shown.

Table S6. Experimental parameters and analytical results for equilibrium partitioning experiments of adipose tissue – see separate excel file.

Experimental parameters include the sampling time points, mass of adipose tissue, mass of PDMS – both at start and at end of the experiment – to determine the amount of co-extracted matrix as well as the calculated mass of lipid, protein, water and residual mass for each time point. The analytical results are shown as total amount of chemical, n_{tot} [mol], and amount of chemical in extract, $n_{extract}$ [mol]. The ratio of C_{PDMS}/C_{lipid} at each time point was calculated with eq. 3 and 4.

Table S7. Experimental parameters and analytical results for uptake kinetic experiments of blood – see separate excel file.

Experimental parameters include the sampling time point, mass of blood, mass of PDMS – both at start and at end of the experiment – to determine the amount of co-extracted matrix as well as the calculated mass of lipid, protein, water and residual mass for each time point. The analytical results are shown as total amount of a given chemical, n_{tot} [mol], and amount of chemical in extract, $n_{extract}$ [mol].

Figure S6. Summary of uptake kinetic curves for each compound measured in liver tissue, brain tissue and blood matrix.

The data from in Table S7 for blood, S9 for liver and S11 for brain tissue. For liver and brain, only $C_{PDMS}(t)/C_{lipid}(t)$ for samples with <40% tissue depletion by uptake into PDMS were used for derivation of uptake kinetics. Different symbols refer to different independent experiments.

Compound	Blood	Liver tissue	Brain tissue
Aldrin	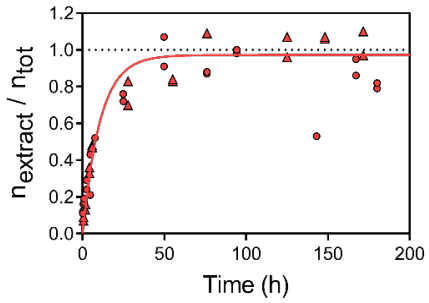	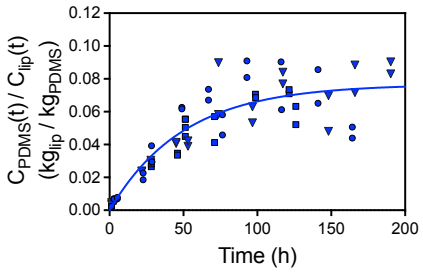	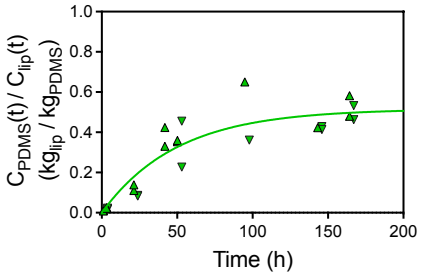
Atrazine	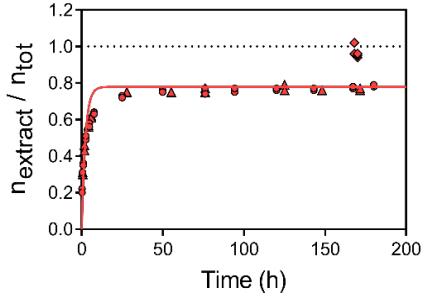	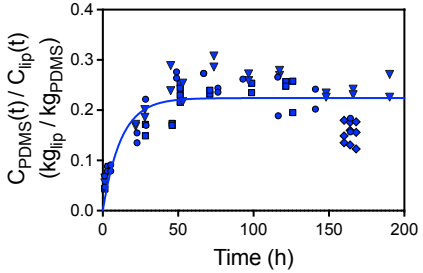	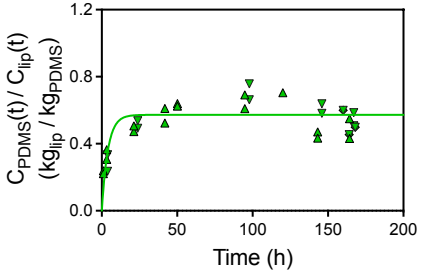

Benzo[*a*]pyrene	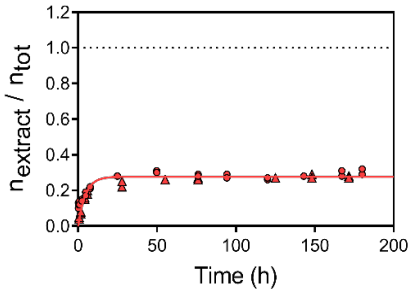	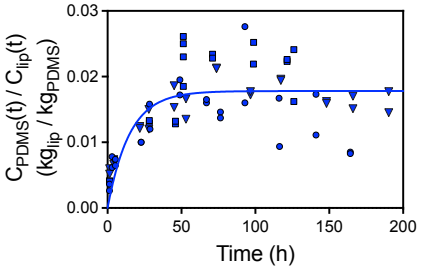	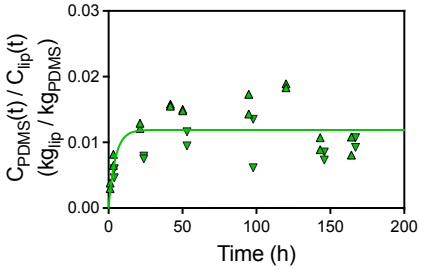
BDE28	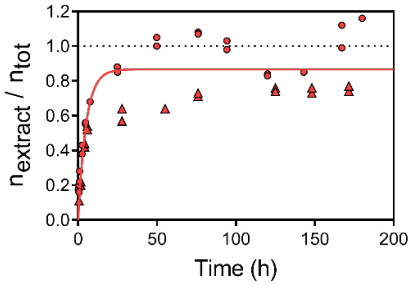	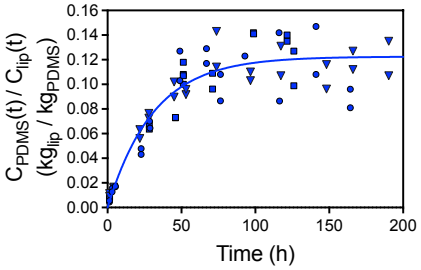	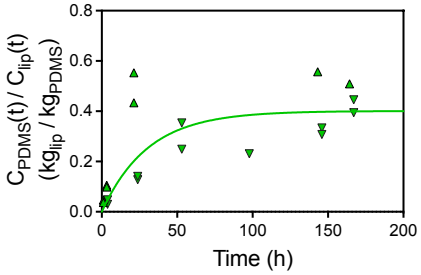
BDE47	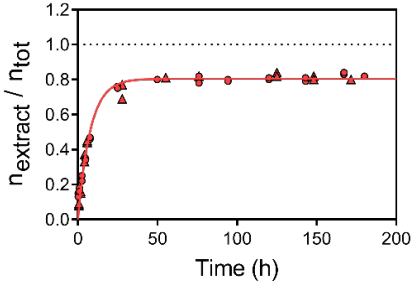	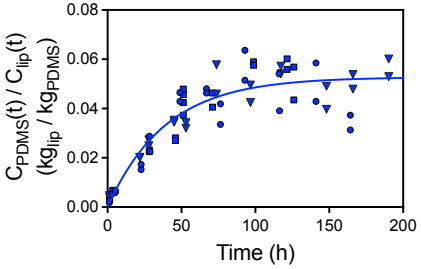	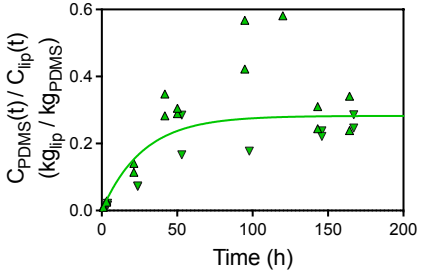

BDE99	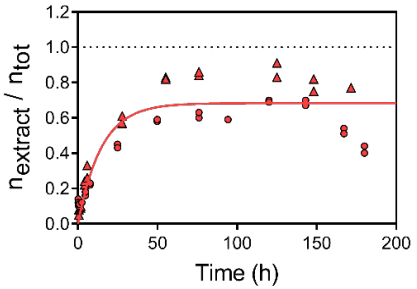	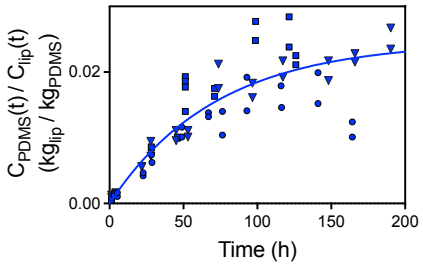	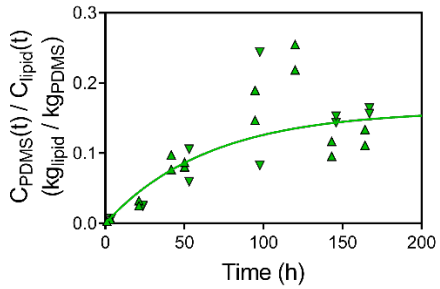
BDE100	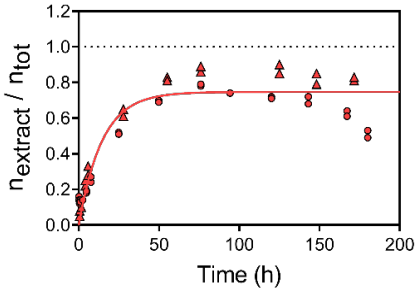	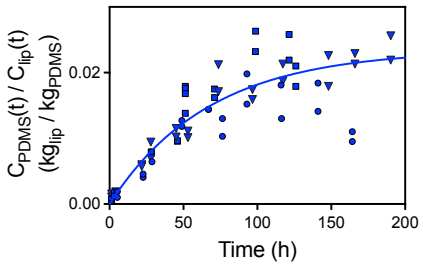	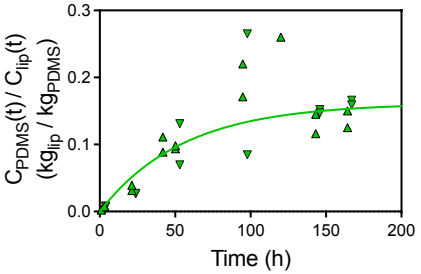
BDE153	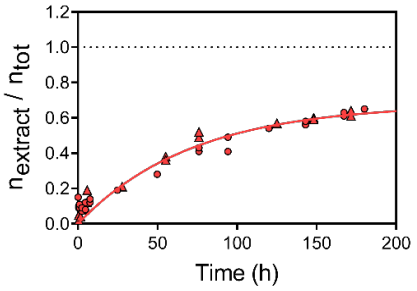	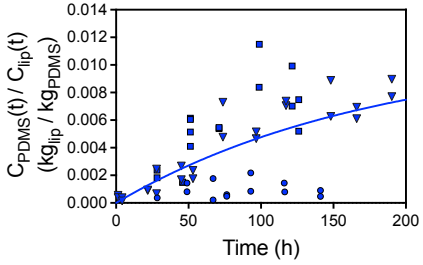	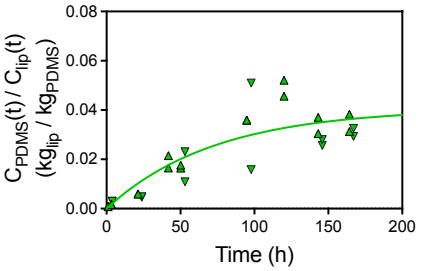

Bromophos-E	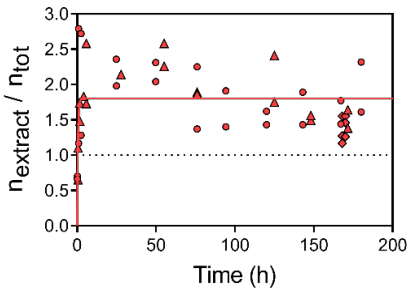	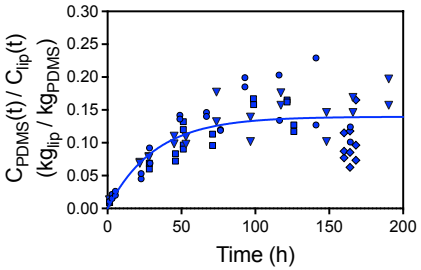	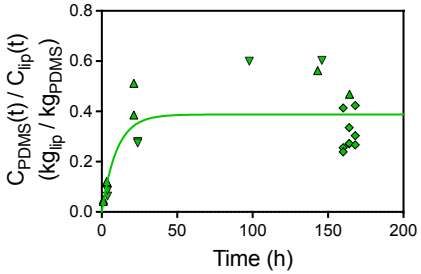
Bromophos-M	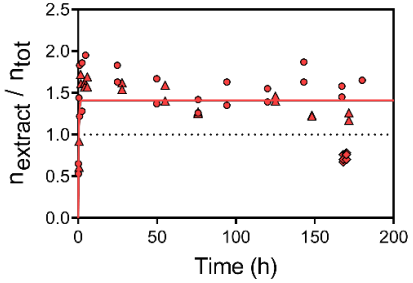	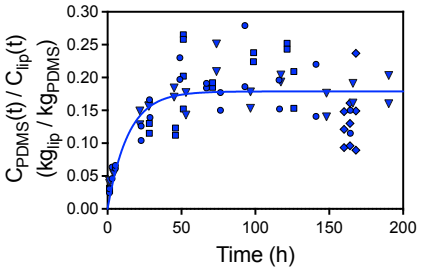	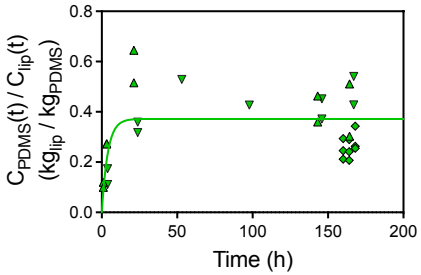
Chlorfenapyr	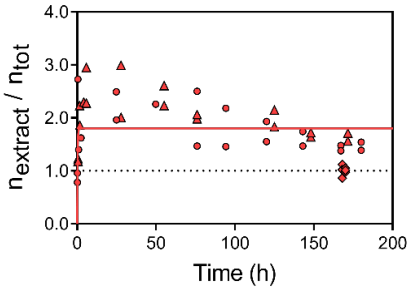	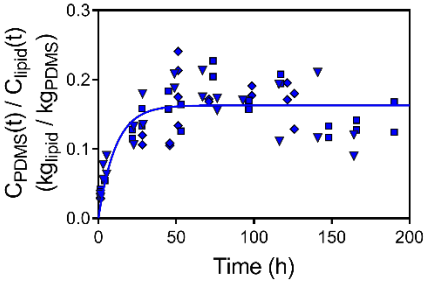	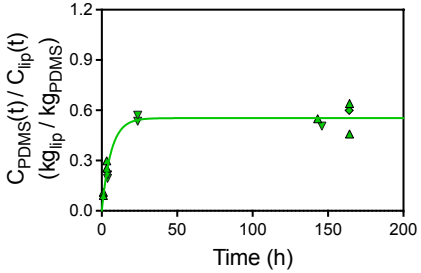

Chlorpyrifos-E	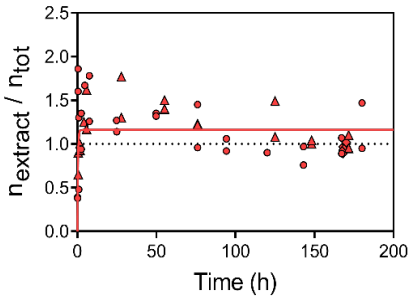	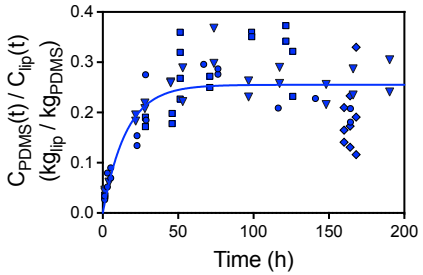	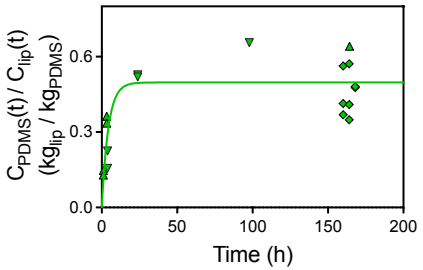
Chlorpyrifos-M	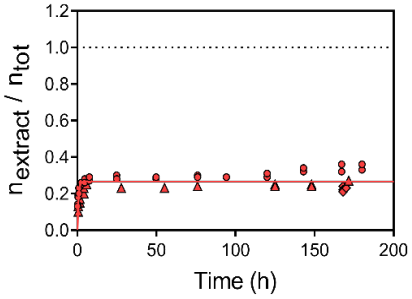	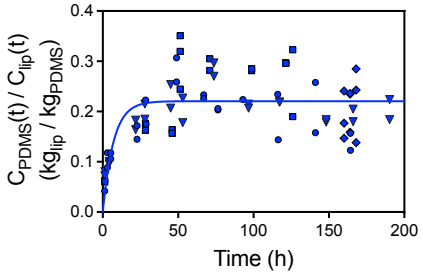	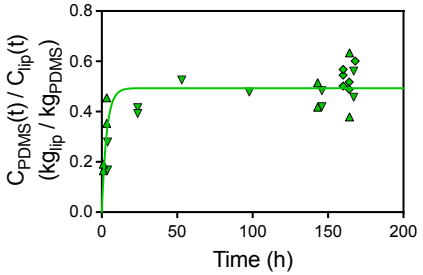
Chrysene	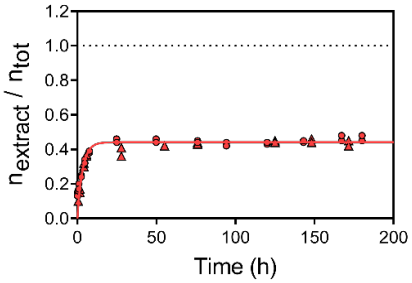	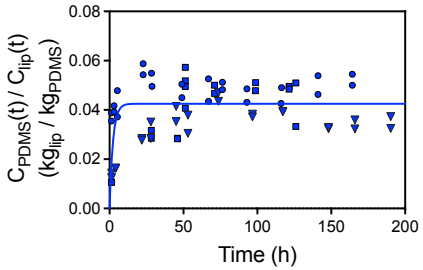	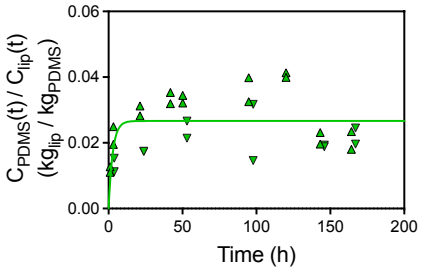

Cybutryne	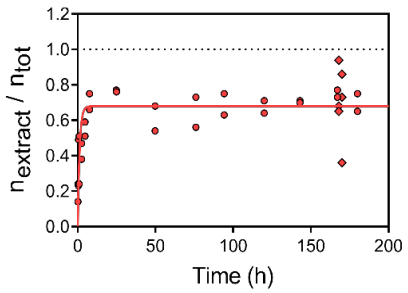	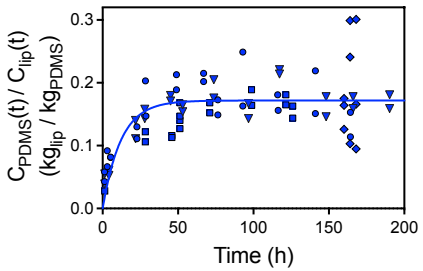	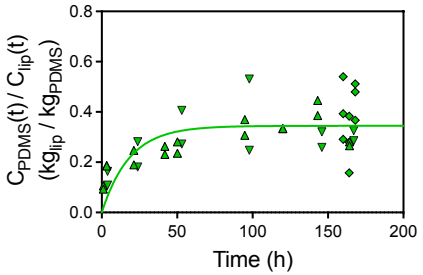
Diazinon	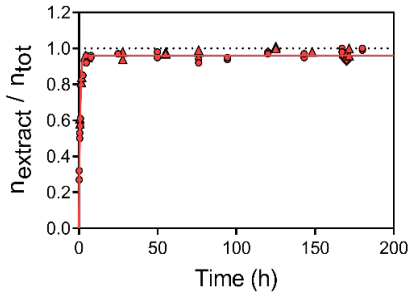	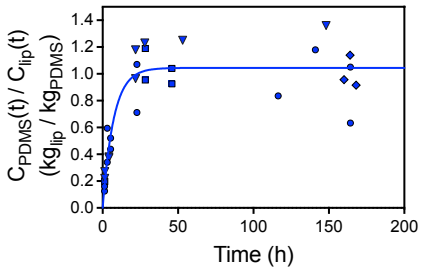	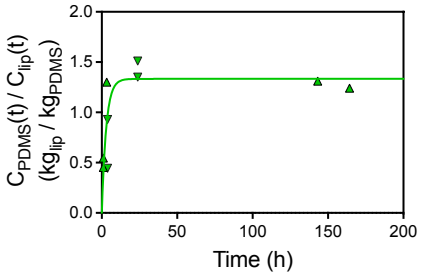
p,p'-DDD	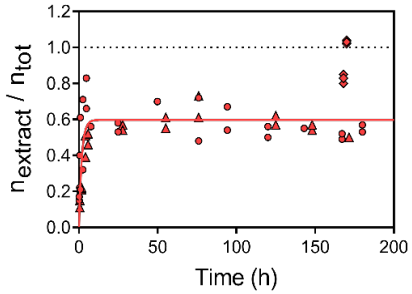	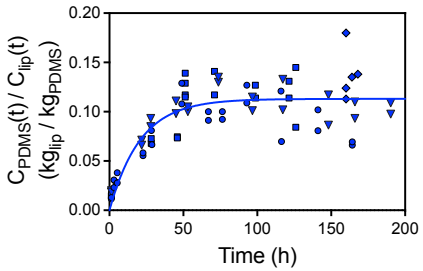	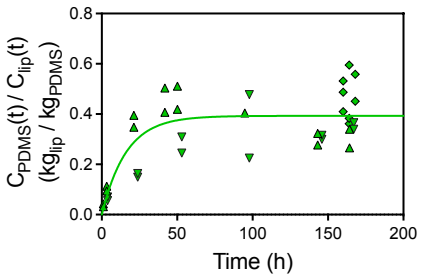

p,p'-DDE	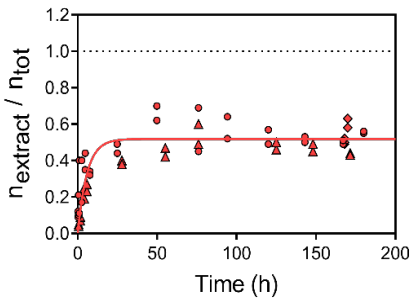	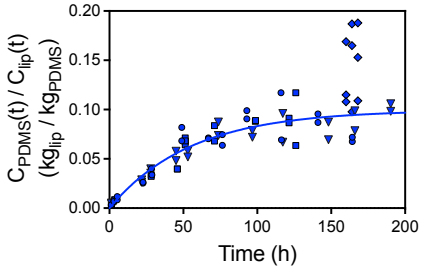	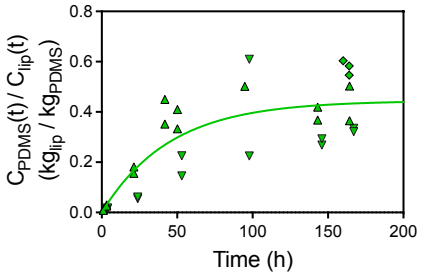
p,p'-DDT	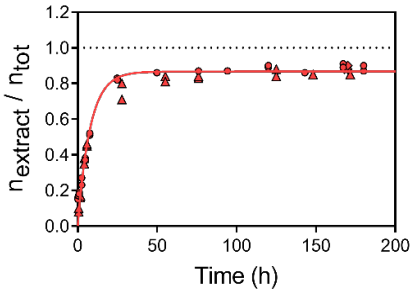	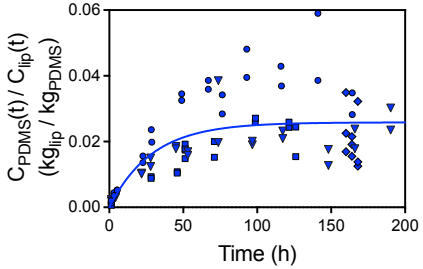	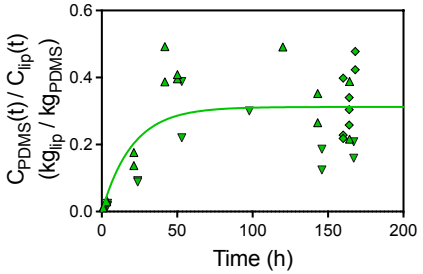
Methoxychlor	No uptake curve recorded.	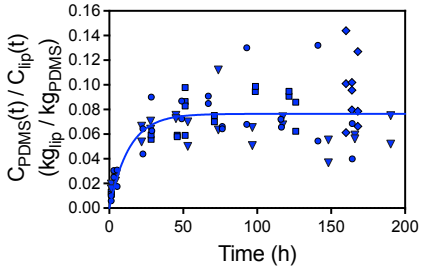	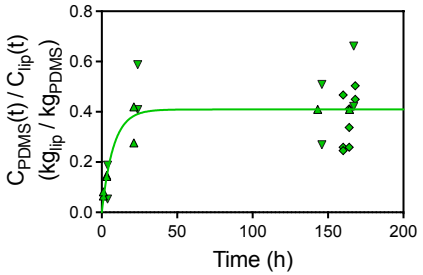

Etofenprox	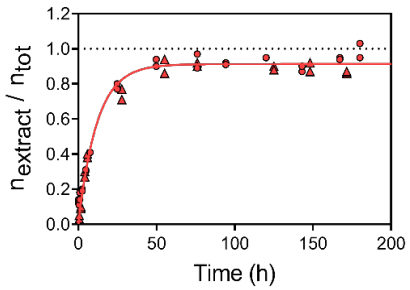	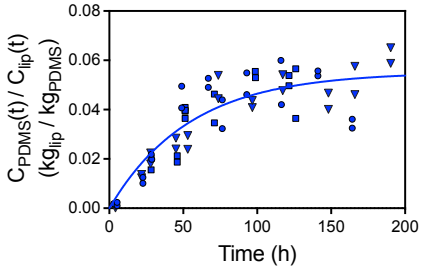	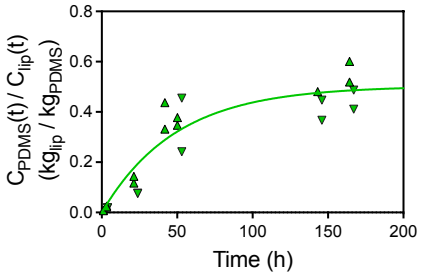
Fipronil	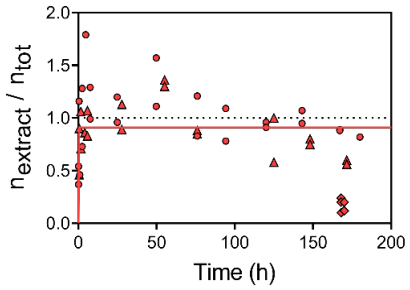	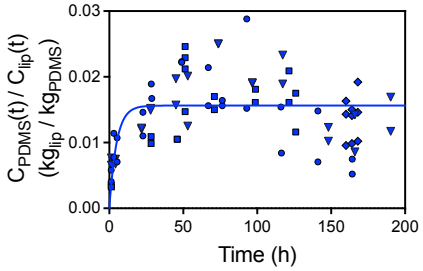	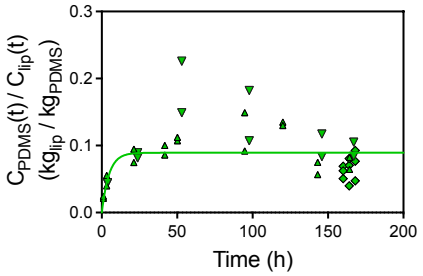
Lindane	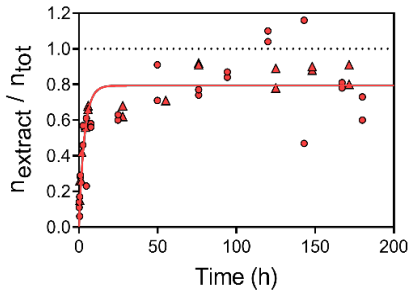	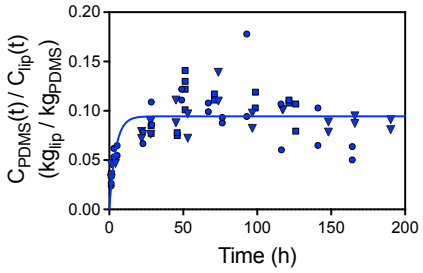	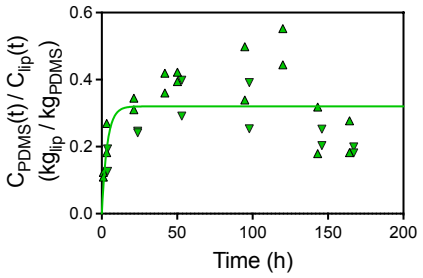

Heptachlor	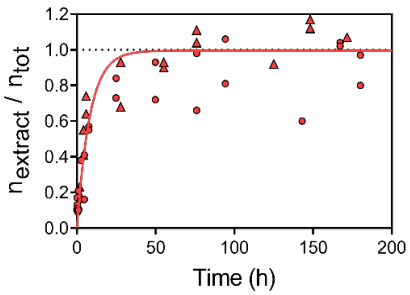	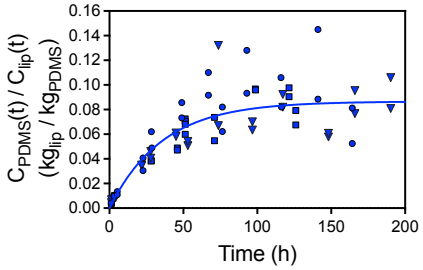	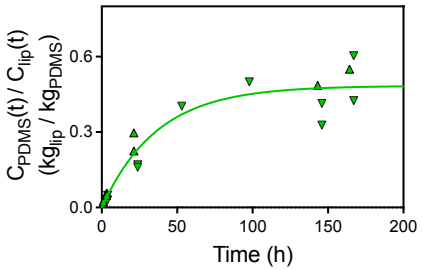
Metolachlor	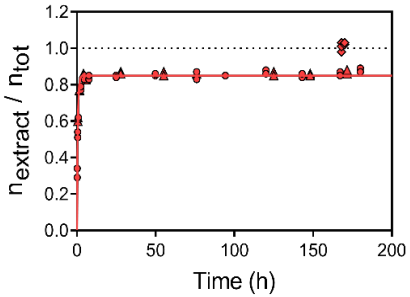	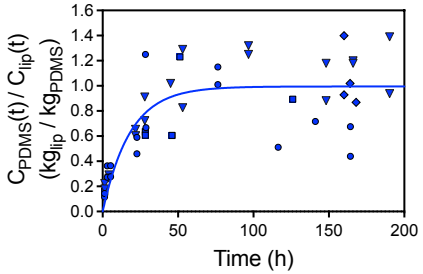	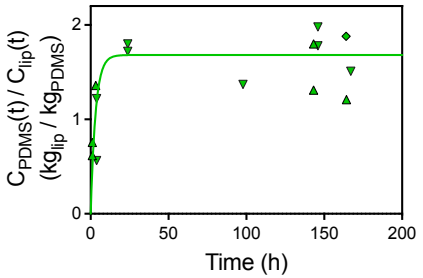
PCB28	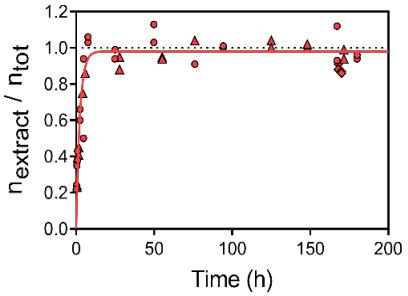	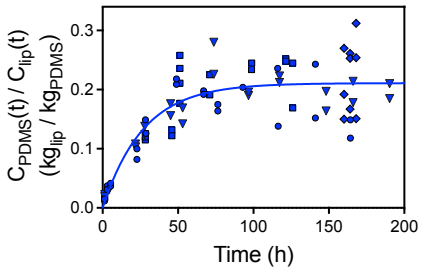	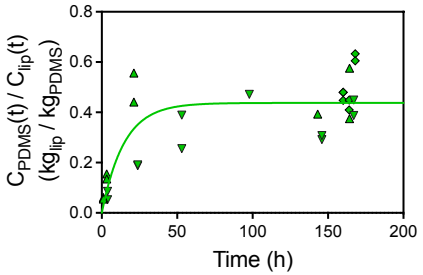

PCB52	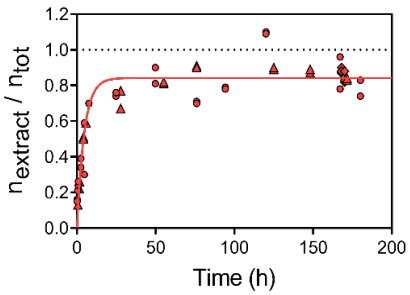	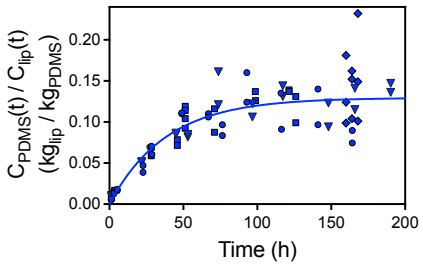	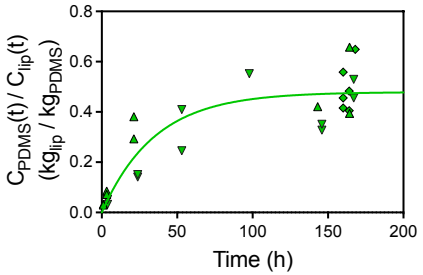
PCB101	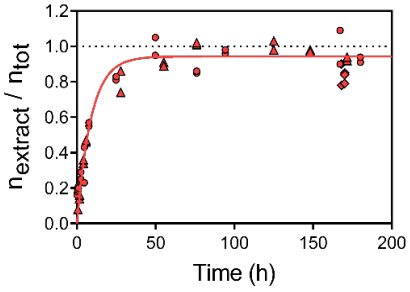	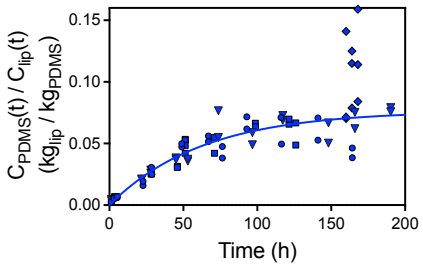	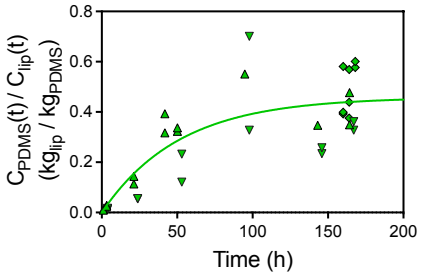
PCB114	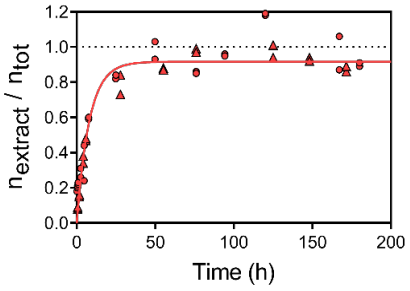	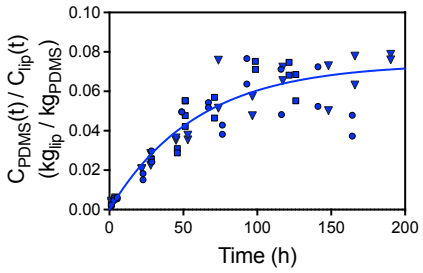	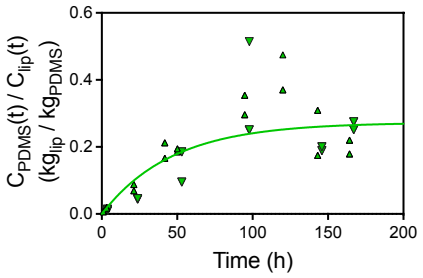

PCB118	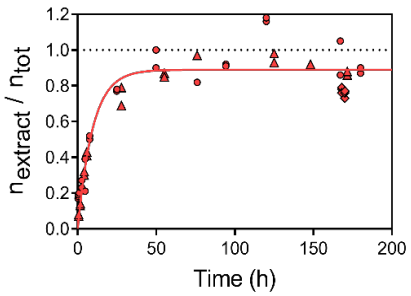	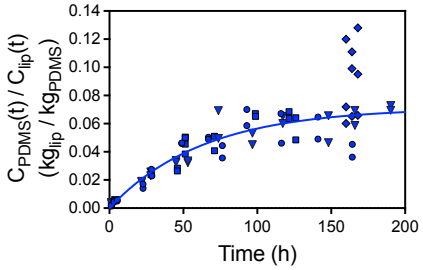	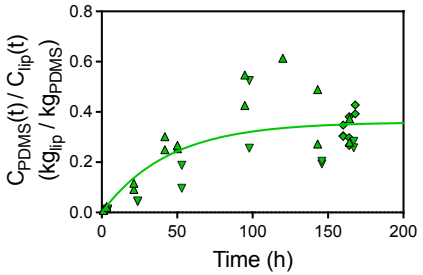
PCB 126	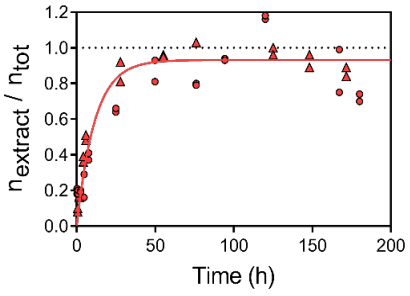	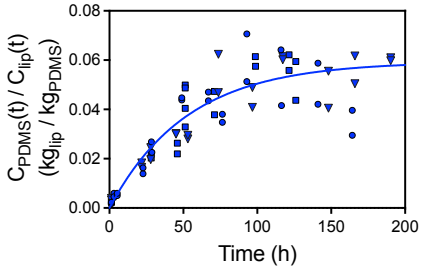	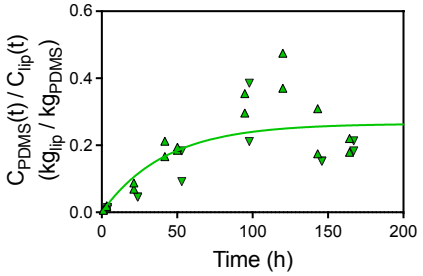
PCB138	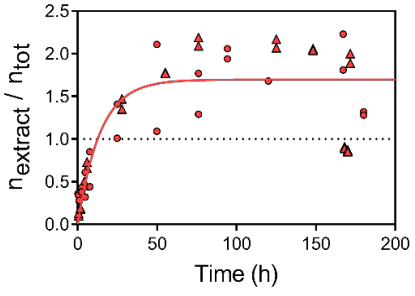	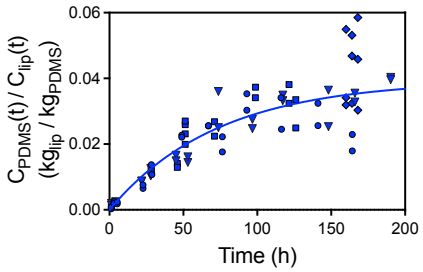	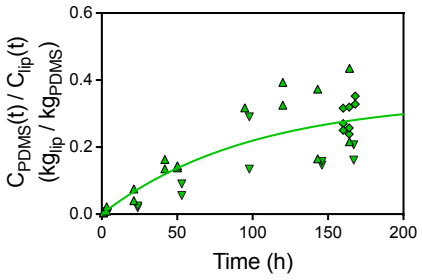

PCB153	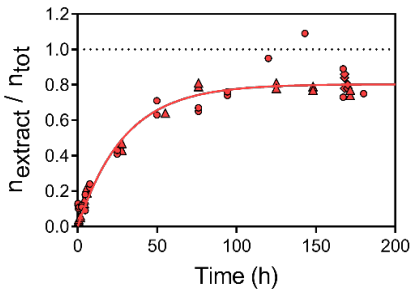	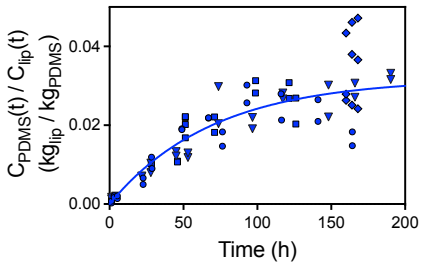	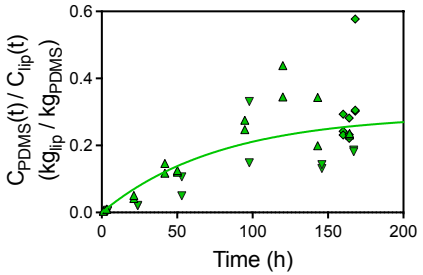
PCB156	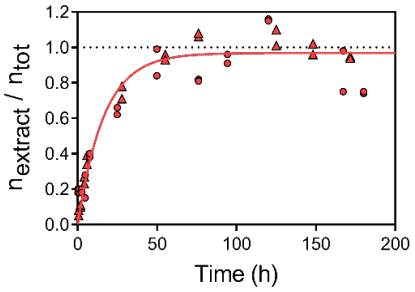	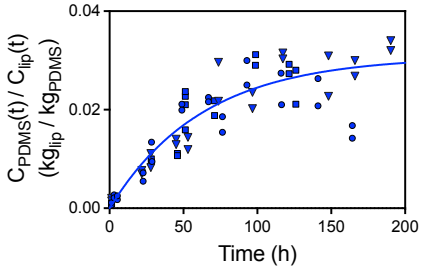	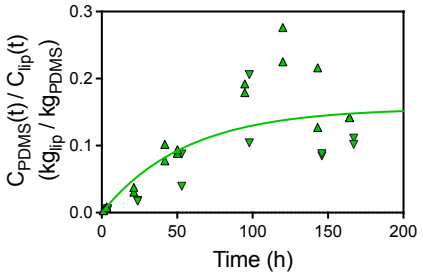
PCB180	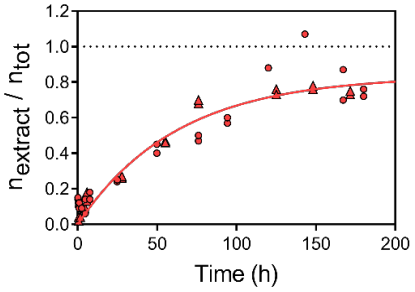	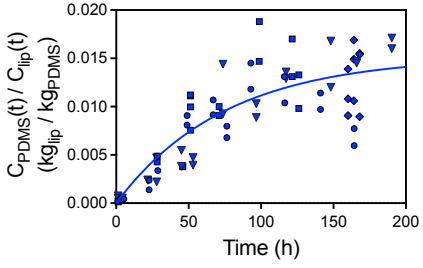	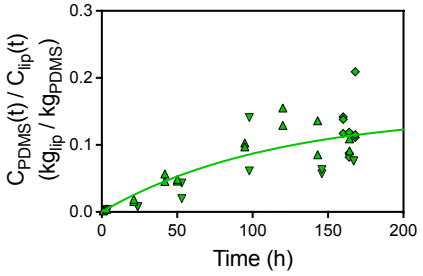

PCB194	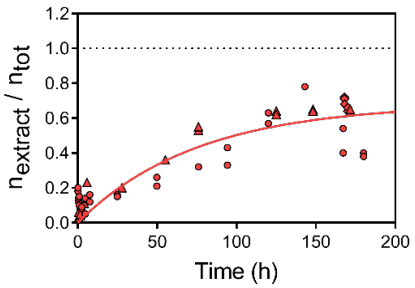	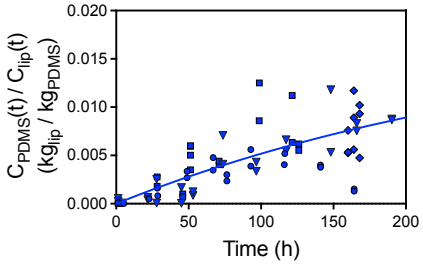	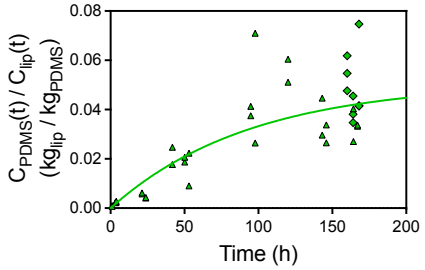
PCB209	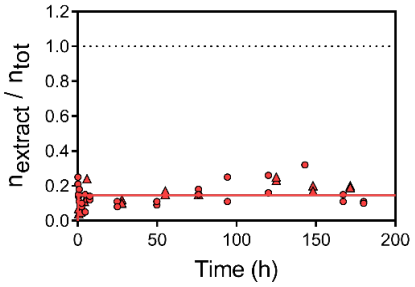	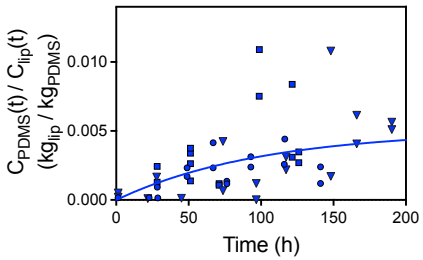	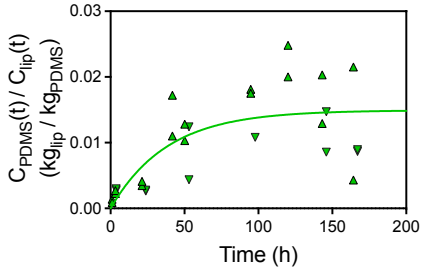
Tris(2-chloroethyl) phosphate	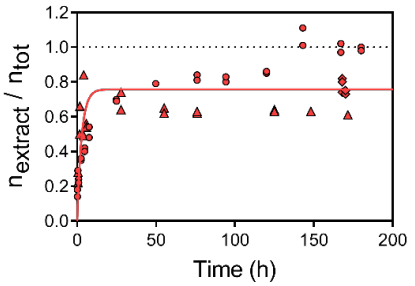	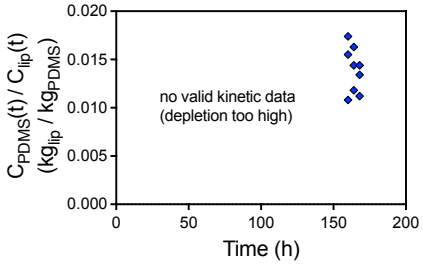	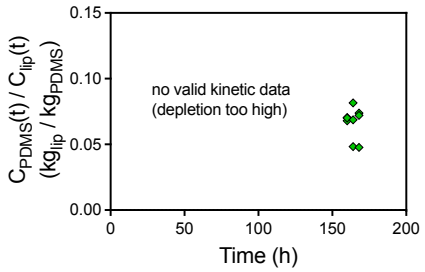

Tris(ortho-methylphenyl) phosphate	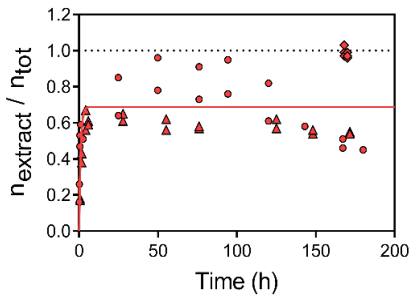	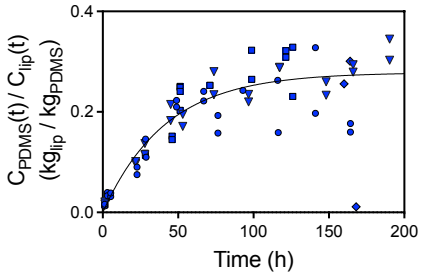	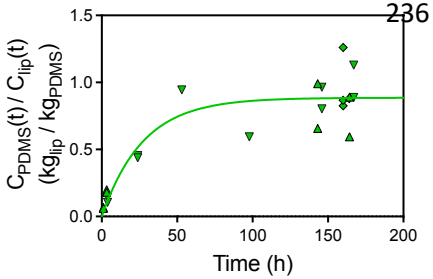
Triphenyl phosphate	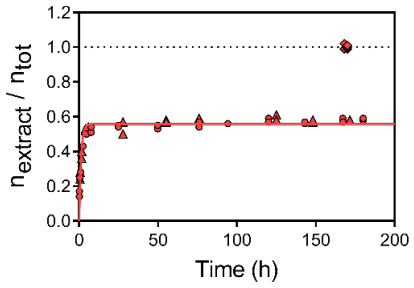	No uptake curve recorded (compound degradation in liver tissue during experiment).	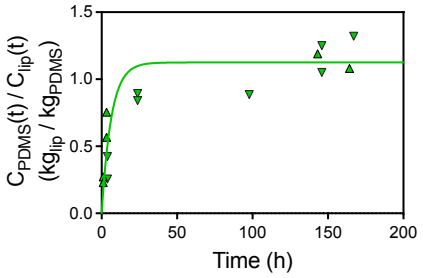

237

Table S8. Summary of PDMS-blood partition experiments – see separate excel file.

Partition constant between PDMS and blood, $K_{PDMS/blood}$ with standard error ($seK_{PDMS/blood}$), uptake rate constant k_{uptake} with standard error (sek_{uptake}) from the fit of the uptake curves (eq. 8) in Figure S6 and statistical fitting parameters (degrees of freedom, R squared, sum of squares and Sy.x). Time for 95% completion of extraction $t_{95\%}$ [h] (= ln(0.05) k_{uptake}). The log$K_{blood/water}$ was derived by dividing the $K_{PDMS/water}$ (Table S1) by the $K_{PDMS/blood}$.

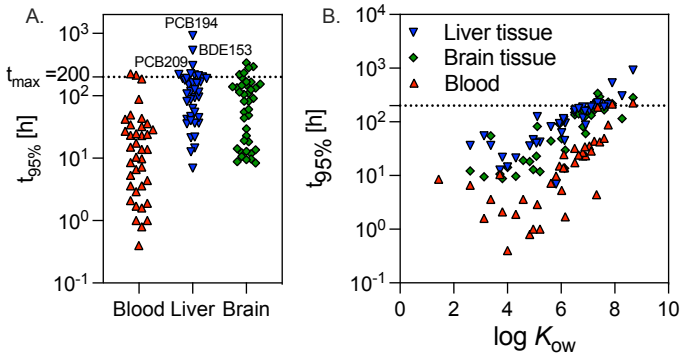

Figure S7. Time to reach equilibrium $t_{95\%}$.

A. Ranges of time to reach equilibrium $t_{95\%}$ ($t_{95\%}$ = ln(0.05) k_{uptake}, Table S8 for blood, Table S9 for liver and Table S10 for brain) indicating the experimental limit of 200h (dotted line), that was mainly exceeded by very hydrophobic chemicals (BDE153, PCB194, PCB209) and B. $t_{95\%}$ as a function of the octanol-water partition constant logK_{ow}.

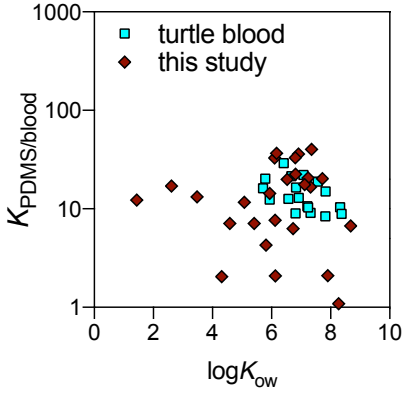

Figure S8. log$K_{PDMS/blood}$ measured in the present study compared to turtle blood.[8]

Table S9. Experimental parameters and analytical results for uptake kinetic experiments of liver – see separate excel file.

Experimental parameters include the sampling time point, mass of liver, mass of PDMS – both at start and at end of the experiment – to determine the amount of co-extracted matrix as well as the calculated mass of lipid, protein, water and residual mass for each time point. The analytical results are shown as total amount of chemical, n_{tot} [mol], and amount of chemical in extract, $n_{extract}$ [mol]. The ratio of $C_{PDMS}(t)/C_{lipid}(t)$ at each time point was calculated with eq. 3 and 4. Only $C_{PDMS}(t)/C_{lipid}(t)$ for samples with <40% depletion of liver tissue by uptake into PDMS were used for derivation of uptake kinetics in Figure S6.

Table S10. Summary of results of uptake kinetics in liver tissue experiments – see separate excel file.

Partition constant between PDMS and lipid, $K_{PDMS/lipid}$, standard error (se) of $K_{PDMS/lipid}$, uptake rate constant k_{uptake}, standard error (se) of k_{uptake} from fit of eq. 9 in Figure S6 and statistical fitting parameters (degrees of freedom, R squared, sum of squares and Sy.x). Time for 95% completion of extraction $t_{95\%}$ [h] (= ln(0.05) k_{uptake}). The log$K_{lipid/water}$ for liver was derived by dividing the $K_{PDMS/water}$ (Table S1) by the $K_{PDMS/lipid}$.

Table S11. Experimental parameters and analytical results for uptake kinetic experiments of brain – see separate excel file.

Experimental parameters include the sampling time point, mass of brain, mass of PDMS – both at start and at end of the experiment – to determine the amount of co-extracted matrix as well as the calculated mass of lipid, protein, water and residual mass for each time point. The analytical results are shown as total amount of chemical, n_{tot} [mol], and amount of chemical in extract, $n_{extract}$ [mol]. The ratio of $C_{PDMS}(t)/C_{lipid}(t)$ at each time point was calculated with eq. 3 and 4. Only $C_{PDMS}(t)/C_{lipid}(t)$ for samples with <40% depletion of brain tissue by uptake into PDMS were used for derivation of uptake kinetics in Figure S6.

Table S12. Summary of results of uptake kinetics in brain tissue experiments – see separate excel file.

Partition constant between PDMS and lipid, $K_{PDMS/lipid}$, standard error (se) of $K_{PDMS/lipid}$, uptake rate constant, k_{uptake}, standard error (se) of k_{uptake} from fit of eq. 9 in Figure S6 and statistical fitting parameters (degrees of freedom, R squared, sum of squares and Sy.x). Time for 95% completion of extraction $t_{95\%}$ [h] (= ln(0.05) k_{uptake}). The log$K_{lipid/water}$ for brain was derived by dividing the $K_{PDMS/water}$ (Table S1) by the $K_{PDMS/lipid}$.

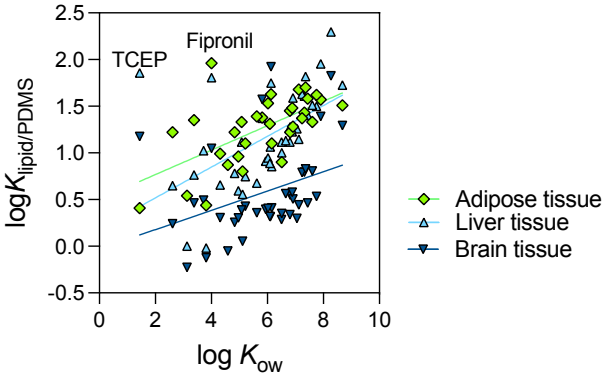

Figure S9. Subtle increase of log$K_{lipid/PDMS}$ (Table 2) with logK_{ow}.

log$K_{lipid/PDMS}$(adipose tissue) = 0.13 x logK_{ow} + 0.51, r^2 = 0.37, n = 40, F = 18)

log$K_{lipid/PDMS}$(liver) = 0.16 x logK_{ow} + 0.19, r^2 = 0.28, n = 39, F = 15)

log$K_{lipid/PDMS}$(brain) = 0.10 x logK_{ow} – 0.03, r^2 = 0.13, n = 40, F = 0)

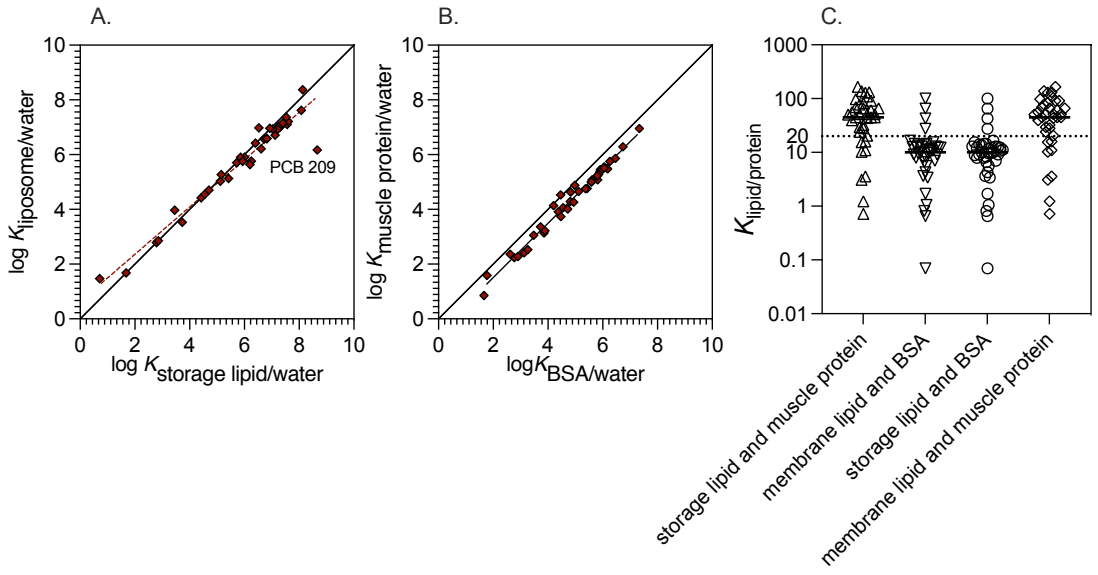

289

290 **Figure S10. Uncertainty analysis of the mass balance model**

291 Variability and uncertainty of (A) relationship between $K_{lipid/w}$ of different lipid surrogates, (B) relationship
292 between $K_{protein/w}$ of different protein surrogates and (C) the $K_{lipid/protein}$ calculated with different
293 combinations of $K_{lipid/w}$ and $K_{protein/w}$.

294

295 **Table S13. Experimental parameters and analytical and bioassay results for uptake kinetic experiments**
296 **of liver in static versus stirred setup with spiked PCB126 – see separate excel file.**

297 Experimental parameters include the sampling time point, mass of liver, mass of PDMS – both at start and
298 at end of the experiment – to determine the amount of coextracted matrix. The analytical results are
299 shown as total amount of PCB126, n_{tot} [mol], and amount of PCB126 in extract, $n_{extract}$ [mol], as well as the
300 effect concentration of the extract in the bioassays EC_{10} in units of relative enrichment factor (REF, kg_{PDMS}
301 $L_{bioassay}^{-1}$) and converted to PCB126 equivalent concentrations PCB126-EQ using the EC_{10} of PCB126 of 9.94
302 ± 0.49 nM.

303

References

1. Ulrich, N.; Endo, S.; Brown, T. N.; Watanabe, N.; Bronner, G.; Abraham, M. H.; Goss, K.-U., UFZ-LSER database v 3.2.1 [Internet], Leipzig, Germany, Helmholtz Centre for Environmental Research-UFZ. 2017 [accessed on 05.02.2021]. Available from http://www.ufz.de/lserd. **2021**.
2. Endo, S.; Bauerfeind, J.; Goss, K.-U., Partitioning of Neutral Organic Compounds to Structural Proteins. *Environ. Sci. Technol.* **2012,** *46*, 12697-12703.
3. Endo, S.; Escher, B. I.; Goss, K. U., Capacities of Membrane Lipids to Accumulate Neutral Organic Chemicals. *Environ. Sci. Technol.* **2011,** *45*, 5912-5921.
4. Endo, S.; Goss, K. U., Serum Albumin Binding of Structurally Diverse Neutral Organic Compounds: Data and Models. *Chem. Res. Toxicol.* **2011,** *45*, 2293-2301.
5. Smedes, F., Determination of total lipid using non-chlorinated solvents. *Analyst* **1999,** *124*, 1711-1718.
6. Baumer, A.; Escher, B. I.; Landmann, J.; Ulrich, N., Direct sample introduction GC-MS/MS for quantification of organic chemicals in mammalian tissues and blood extracted with polymers without clean-up. *Anal Bioanal Chem* **2020,** *412*, 7295-7305.
7. Jahnke, A.; Mayer, P.; Broman, D.; McLachlan, M. S., Possibilities and limitations of equilibrium sampling using polydimethylsiloxane in fish tissue. *Chemosphere* **2009,** *77*, 764-770.
8. Jin, L.; Escher, B. I.; Limpus, C. J.; Gaus, C., Coupling passive sampling with in vitro bioassays and chemical analysis to understand combined effects of bioaccumulative chemicals in blood of marine turtles. *Chemosphere* **2015,** *138*, 292-299.
9. Neale, P. A.; Altenburger, R.; Ait-Aissa, S.; Brion, F.; Busch, W.; de Aragão Umbuzeiro, G.; Denison, M. S.; Du Pasquier, D.; Hilscherova, K.; Hollert, H.; Morales, D. A.; Novac, J.; Schlichting, R.; Seiler, T.-B.; Serra, H.; Shao, Y.; Tindall, A. J.; Tollefsen, K. E.; Williams, T. D.; Escher, B. I., Development of a bioanalytical test battery for water quality monitoring: Fingerprinting identified micropollutants and their contribution to effects in surface water. *Water Res.* **2017,** *123*, 734-750.
10. Escher, B. I.; Glauch, L.; Konig, M.; Mayer, P.; Schlichting, R., Baseline Toxicity and Volatility Cutoff in Reporter Gene Assays Used for High-Throughput Screening. *Chem Res Toxicol* **2019,** *32*, 1646-1655.
11. Reiter, E. B.; Jahnke, A.; Konig, M.; Siebert, U.; Escher, B. I., Influence of Co-Dosed Lipids from Biota Extracts on the Availability of Chemicals in In Vitro Cell-Based Bioassays. *Environ. Sci. Technol.* **2020,** *54*, 4240-4247.
12. Escher, B. I.; Neale, P. A.; Villeneuve, D. L., The advantages of linear concentration-response curves for in vitro bioassays with environmental samples. *Environ Toxicol Chem* **2018,** *37*, 2273-2280.

336 13. Reichenberg, F.; Smedes, F.; Jonsson, J. A.; Mayer, P., Determining the chemical activity of
337 hydrophobic organic compounds in soil using polymer coated vials. *Chem. Cent. J.* **2008,** *2*, 8.

338